IEEE Access
Multidisciplinary | Rapid Review | Open Access Journal

Received 28 June 2022, accepted 3 August 2022, date of publication 16 August 2022, date of current version 31 August 2022.

Digital Object Identifier 10.1109/ACCESS.2022.3198988

RESEARCH ARTICLE

EEG Signal Processing for Alzheimer's Disorders Using Discrete Wavelet Transform and Machine Learning Approaches

KHALIL ALSHARABI, YASSER BIN SALAMAH, AKRAM M. ABDURRAQEEB, MAJID ALJALAL, AND FAHD A. ALTURKI

Department of Electrical Engineering, College of Engineering, King Saud University, Riyadh 800-11421, Saudi Arabia

Corresponding author: Khalil Alsharabi (kabdulghani@ksu.edu.sa)

This work was supported by the King Saud University, Riyadh, Saudi Arabia, under Grant RSP-2021/252.

This work involved human subjects or animals in its research. Approval of all ethical and experimental procedures and protocols was granted by the Ethics Committee for the Analysis of Research Projects - CAPPesq of the Clinical Board of Hospital das Clinicas and of the Faculty of Medicine of the University of São Paulo (under Application No. 0630/09, and performed in line with the Study of EEG Wavelets Analysis in Patients With Probable Alzheimer's Disease).

ABSTRACT The most common neurological brain issue is Alzheimer's disease, which can be diagnosed using a variety of clinical methods. However, the electroencephalogram (EEG) is shown to be effective in detecting Alzheimer's disease. The purpose of this research is to develop a computer-aided diagnosis system that can diagnose Alzheimer's disease using EEG data. In the present study, a band-pass elliptic digital filter was used to eliminate interference and disturbances from the EEG dataset. Next, the Discrete Wavelet Transform (DWT) technique has been employed to decompose the filtered signal into its frequency bands in order to extract the features of EEG signals. Then, different signal features such as logarithmic band power, standard deviation, variance, kurtosis, average energy, root mean square, and Norm have been integrated into the DWT technique to generate the feature vectors and improve the diagnosis performance. After that, nine machine learning approaches have been investigated to classify EEG features into their corresponding classes: linear discriminant analysis (LDA), quadratic discriminant analysis (QDA), support vector machine (SVM), Naïve bayes (NB), k-nearest neighbor (KNN), decision tree (DT), extreme learning machine (ELM), artificial neural network (ANN), and random forests (RF). Finally, the performance of the different proposed machine learning approaches have been compared and evaluated by computing the sensitivity, specificity, overall diagnosis accuracy, and area under the receiver operating characteristic (ROC) curves and plotting the ROC curves and confusion matrices for five classification problems. These investigations aim to compare the proposed approaches and recommend the best combination method for the diagnosis of Alzheimer's disorders. According to the results, the KNN classifier achieved an average classification accuracy of 99.98% with an area under the ROC curve of 100%. Our findings show that the suggested methodologies are an appealing supplementary tool for identifying possible biomarkers to help in the clinical diagnosis of Alzheimer's disease.

INDEX TERMS Alzheimer's disease, artificial neural network, average energy, decision tree, discrete wavelet transform, electroencephalogram, extreme learning machine, K-nearest neighbor, linear discrimination analysis, logarithmic band power, Naïve Bayes, quadratic discriminant analysis, random forests, support vector machines.

I. INTRODUCTION

Neurological brain disorders include any disorders in the brain or another part of the nervous system and Alzheimer's disease is one of the most common neurological brain disorders in the world. Alzheimer's disease (AD) is a type of neurodegenerative disease characterized by progressive loss of neurological, mental, and cognitive functions, including memory, changes in judgment, behavior, and emotions [1], [2], [3] and it represents the major cause of dementia because

The associate editor coordinating the review of this manuscript and approving it for publication was Thomas Canhao Xu.

it corrupts the neurons of the brain and particularly the axons, by destroying the neurotransmitters that are important for memory storage and message transmission to the brain [4]. According to World Health Organization (WHO) report, neurological disorders are posing a global public health threat by affecting hundreds of millions of people worldwide [5]. In 2005, WHO estimated that dementia affected 0.379% worldwide population, and the prevalence would increase to 0.556% in 2030 [5]. In their recent information [6], 47.5 million people have dementia and Alzheimer's disease may contribute to 60–70% of cases. In 2015, there were approximately 29.8 million people worldwide with AD [7].

Currently, diagnosis of neurological brain disorders is still mainly carried out manually by neurologists or medical experts who are still limited available. In some cases, the neurologists need several hours to make a final diagnosis decision for a single patient. In recent years, the researchers in the multidisciplinary fields of bioengineering and neuroscience have made considerable efforts for enhancing the performance of brain–computer interface (BCI) [8], [9] and developing a computer-aided diagnosis (CAD) system. For this, the researchers use all the information provided by EEG signals because EEG signals have several advantages such as simple, relatively cheaper, more widely available, and high temporal resolution because it reflects the electrical brain activities of neurological disorders. Several signal-processing and machine learning techniques for EEG feature extraction and classification have recently been presented and discussed to develop an early prediction system capable of automatically analyzing brain signals and assisting neurologists in the early prediction of neurological disorders such as Autism Spectrum Disorder (ASD) [10], Epilepsy Disorders (ED) [11], both of autism spectrum disorder and epilepsy disorders [12], [13], [14], Parkinson's disease [15] and Alzheimer disorders (AD).

As a result, numerous researchers have started working on computer systems that can identify Alzheimer's disease by studying brain signals from patients. For example, Morabito *et al.* [16] proposed utilizing Deep Learning's representational power on Convolutional Neural Networks (CNN) to build appropriate sets of EEG signal features that can then be used to classify AD EEG patterns. The proposed approach employs a sequence of convolutional-subsampling layers to generate a multivariate assembly of unique patterns, which is then utilized to classify sets of EEG from various participants. The proposed approach had an accuracy of 80%. Cassani *et al.* [17] reported an automated EEG-based AD diagnostic system based on an automated artifact removal (AAR) algorithm and a low-density (7-channel) EEG setup. Following AAR, common EEG parameters including spectral power and coherence, as well as amplitude-modulation properties, are computed. A support vector machine (SVM) is used to classify the collected features. The proposed diagnostic system had a maximum accuracy of 91.4%. Ieracitano *et al.* [18] provided a multi-modal machine learning-based strategy for automatic classification of EEG recordings in dementia in their paper. They employed a Multi-Layer Perceptron (MLP) classifier based on Auto-Encoder (AE), Logistic Regression (LR), and Support Vector Machine (SVM), as well as the Continuous Wavelet Transform (CWT) approach with the bispectrum (BiS) feature for feature extraction (SVM). Their proposed approach has a 97 percent accuracy rate. Trambaiolli *et al.* [19] used eight distinct feature selection techniques and an SVM classifier to reach an accuracy of 91.18% for EEG spectral readings.

Based on EEG signals, Bevilacqua *et al.* [20] tested numerous classifiers for distinguishing between Normal and individuals with Alzheimer's disease. Support Vector Machines Recursive Features Elimination (SVMRFE), Principal Component Analysis (PCA), and a unique method based on the correlation are the three major procedures utilized to conduct feature dimensionality reduction. Five classifiers compared two different SVM configurations and three distinct Error Back Propagation Multi-Layer Perceptron Artificial Neural Network configurations (MLP-ANN). Their method has an 86% diagnosing accuracy rate. Fiscon [21] provided a diagnostic system that employed tree-based classifiers and used Fourier and wavelet analysis as feature extraction methods (J48). The proposed method yielded a maximum diagnostic accuracy of 92%. The power and functional connectivity of cortical sources in the frontal, central, parietal, occipital, temporal, and limbic areas were estimated using Exact low-resolution brain electromagnetic tomography (eLORETA) by Triggiani *et al.* [22]. The authors used an ANN classifier to get a 75.5% diagnostic accuracy. Another recent study by Amezquita-Sanchez *et al.* [23] suggested using the integrated multiple signal classification and empirical wavelet transform (MUSIC-EWT), different nonlinear features such as fractality dimension (FD) from chaos theory, and a classification algorithm, the enhanced probabilistic neural network (EPNN) model, to diagnose AD using EEG-based computer-aided diagnosis. The proposed method had a diagnostic accuracy of 90.3%.

Recently, Perez-Valero *et al.* [24] developed a computer-aided system for Alzheimer's disease diagnosis. In their study, EEG signals were used to construct the matrix of connections and a convolutional neural network is used for classification. Their system achieved maximum accuracy reach to 62% but achieved 75% for the classification of raw EEG data with Alzheimer's disease data. Araújo *et al.* [25] used the wavelet packet technique for feature extraction and classical machine learning approaches and convolutional neural network for classification. Their system achieved a maximum accuracy reach to 84.2%. In the study of Alessandrini *et al.* [26], robust principal component analysis (RPCA) and multi-scale principal component analysis (MSPCA) were used for pre-processing. The principal component analysis (PCA) technique is used for feature extraction and recurrent neural network (RNN) for classification. The system achieved a maximum accuracy reach to 94.6%.

It is important to mention that the diagnosis stage of Alzheimer's disorders is the most important stage for completing the treatment and healthcare and it is important to

choose the perfect clinical diagnosis system. Most of the studies mentioned in the literature employed methods related to extracting the features and classifying them into their corresponding classes. However, no study has used a suitable combination of methods to decompose the EEG signals, extract the features, and classify those features for developing the perfect clinical diagnosis system for Alzheimer's disease. Accordingly, in this study, we developed a computer-aided diagnostic system for diagnosing and early detecting of Alzheimer's diseases. Different combination methods for feature extraction and classification were investigated for the development of the perfect clinical diagnosis system to assist neurologists in automatically, rapidly, and accurately diagnosing Alzheimer's disorders.

After reading the EEG dataset, First, its noises were filtered in the pre-processing stage using the band-pass elliptic filter. Then, the DWT technique was used in order to decompose the filtered EEG signal into its frequency bands. Next, several statistical features such as logarithmic band power, standard deviation, variance, kurtosis, average energy, root mean square, and Norm have been investigated to combine with DWT to form the features matrix and improve the diagnosis performance. After that, for further investigation, nine machine learning techniques have been employed: Linear Discriminant Analysis, Quadratic Discriminant Analysis, Support Vector Machine, Naïve Bayes, K-Nearest Neighbor, Decision Tree, Extreme Learning Machine, Artificial Neural Network, and Random Forest. The diagnosis performances have been evaluated for five classification problems investigated from three dataset groups. The diagnosis performance has been evaluated by computing the classification accuracies, areas under the curves of receiver operating characteristic (ROC) curves, sensitivity, and specificity. These investigations aim to compare the proposed techniques and recommend the best combination method for the diagnosis and early detection of Alzheimer's disorders. The results of the proposed diagnosis system have been presented and discussed below.

The remainder of this paper is organized as follows. Section II describes the EEG dataset that is utilized in this study, feature extraction, and classification techniques. Section III is dedicated to presenting the results and the discussion. Finally, the conclusion and future work prospects are presented in Section IV.

ABBREVIATION

AAR	Automated Artifact Removal.
AD	Alzheimer's disease.
AE	Average energy.
ANN	Artificial Neural Network.
ASD	Autism Spectrum Disorders.
AuE	Auto-Encoder.
BCI	Brain–Computer Interface.
BiS	Bispectrum.
CAD	Computer Aided Diagnosis.
CNN	Convolutional Neural Networks.
CWT	Continuous Wavelet Transform.
DT	Decision Tree.
DWT	Discrete Wavelet Transform.
ED	Epilepsy Disorders.
EEG	Electroencephalogram.
ELM	Extreme Learning Machine.
eLORETA	Exact low-resolution brain electromagnetic tomography.
EPNN	Enhanced Probabilistic Neural Network.
EWT	Empirical Wavelet Transform.
FD	Fractality Dimension.
IIR	Infinite Impulse Response.
KNN	K-Nearest Neighbor.
KUR	Kurtosis.
LBP	Logarithmic band power.
LDA	Linear Discriminant Analysis.
LR	Logistic Regression.
MLP-ANN	Multi-Layer Perceptron Artificial Neural Network.
MSE	Multiscale Sample Entropy.
MSPCA	Multi-Scale Principle Component Analysis.
NB	Naïve Bayes.
NO	Norm.
PCA	Principal Component Analysis.
QDA	Quadratic Discriminant Analysis.
QSE	Quadratic Sample Entropy.
RF	Random Forests.
RMS	Root Mean Square.
rMSE	refined Multiscale Spectral Entropy.
RNN	Recurrent Neural Network.
ROC	Receiver Operating Characteristic.
RPCA	Robust Principle Component Analysis.
StD	Standard Deviation.
SVM	Support Vector Machine.
SVMRFE	Support Vector Machines Recursive Features Elimination.
VAR	Variance.
WHO	World Health Organization.
wICA	wavelet enhanced Independent Component Analysis.

II. MATERIALS AND METHODS

In this section, the utilized EEG datasets have been described and the proposed methods that are used for processing the EEG signals have been described as well. To develop a CAD system for medical neurological brain diseases diagnosis, four main steps have been followed as shown in Figure 1, namely, EEG data reading, pre-processing, feature extraction, and classification and decision making. First, The collected EEG signals are processed and treated using a pre-processing block to eliminate any noise and interference in the brain patterns. An elliptic band-pass filter is used to efficiently limit the signals to a frequency between 0.1 and 60 Hz. Next, the filtered signal has been introduced to the DWT technique to decompose the filtered signal to its frequency subbands (Delta, Theta, Alpha, Beta, and Gamma). After that,

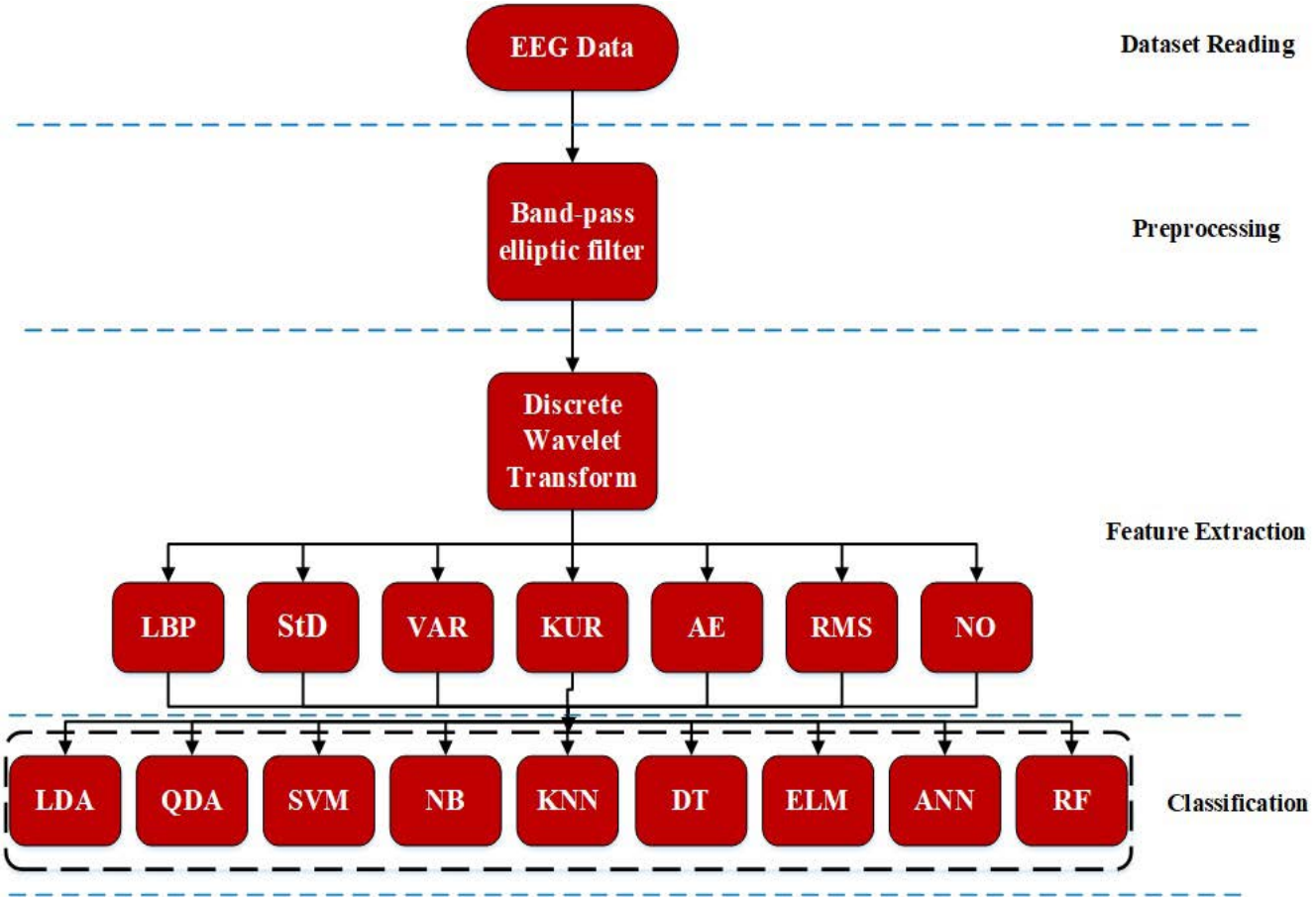

FIGURE 1. Generic block diagram of proposed CAD system for medical neurological brain disease diagnosis based on DWT.

the feature vectors were extracted by computing the several statistical features: logarithmic band power (LBP), standard deviation (StD), variance (VAR), kurtosis (KUR), average energy (AE), root mean square (RMS) and norm (NO) of the EEG frequency sub-bands. The extracted features have been classified by different machine learning approaches such as Linear Discriminant Analysis (LDA), Quadratic Discriminant Analysis (QDA), Support Vector Machine (SVM), Naïve Bayes (NB), K Nearest Neighbor (KNN), Decision Tree (DT), Extreme Learning Machine (ELM), Artificial Neural Network (ANN) and Random Forest (RF). Finally, all the possible combinations of the proposed approaches were implemented and verified. These proposed methods have been also verified using MATLAB software simulation tools. In the following subsections, each stage has been presented and discussed in more detail, from the data description to the classification process.

A. DATASET DESCRIPTION

1) SUBJECTS

In this study, the datasets of AD patients and control subjects were recorded by the Behavioral and Cognitive Neurology Unit of the Department of Neurology and the Reference Center for Cognitive Disorders at the Hospital das Clinics in Sao Paulo, Brazil. All AD patients and Control subjects were diagnosed and the datasets were recorded by experienced neurologists based on the Brazilian version of the Clinical Dementia Rating (CDR) scale and the Mini-Mental State Examination (MMSE) [27]. The multi-channel EEG datasets were recorded from 86 participants, separated into three groups. There are 35 Control subjects (CS), 16 males and 19 females in the first group (mean age 66.89 years, 8.18 StD). Inclusion criteria for the cognitively Normal cohort were CDR score which is equal to 0 and MMSE greater than or equal to 25 with mean MMSE equal to 28 and standard deviation equal to 2.2 and based on an interview with the individuals, there was no evidence of functional cognitive deterioration prior to recording. According to NINCDS-ADRDA [28] and DSM-IVTR [29] criteria, the second group contains 31 mild-AD patients, 12 males and 19 females (mean age 75.23 years, 5.55 StD). Other inclusion criteria for the mild AD patients group were $0.5 \leq \text{CDR} \leq 1$ and $\text{MMSE} \leq 24$ with mean MMSE equal to 19.48 and standard deviation equal to 3.16. The third group includes 22 moderate AD patients according to DSM-IV-TR, 7 males and 15 females (mean age 73.77 years, 10.16 StD). Inclusion criteria for moderate AD patients group were CDR score equal to 2 and

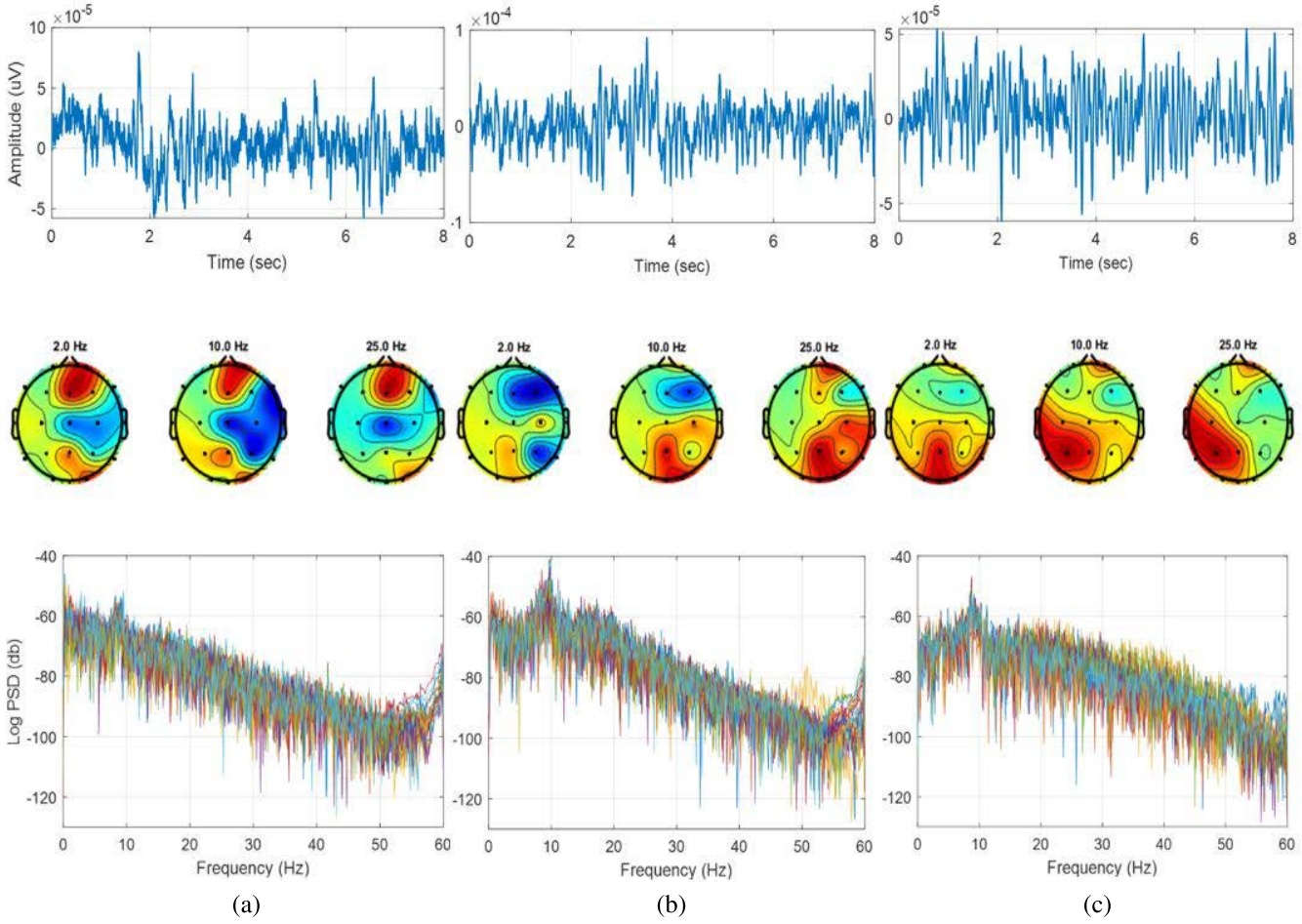

FIGURE 2. EEG signals sample, electrodes maps, and power spectrum density pattern for (a) Control EEG (b) Mild AD EEG, and (c) Moderate AD EEG.

MMSE score $\leq$ 20 with mean MMSE 14.18 and standard deviation equal to 3.69. For inclusion in both AD cohorts (AD1 and AD2) an additional criterion was the presence of functional and cognitive decline over the previous 12 months based on a detailed interview with a knowledgeable informant. Patients from both AD groups were also screened for diabetes mellitus, kidney disease, thyroid disease, alcoholism, liver disease, lung disease, or vitamin B12 deficiency, as these can cause cognitive decline [30]. Table 1 shows the description of the subjects' characteristics.

Figure 2 shows the sample of EEG signals, electrode maps, and EEG power spectrum density with a logarithmic scale for three different datasets: Control, Mild AD, and Moderate AD datasets. the sample of EEG signals is the signals which have been recorded from Fp1 electrode of three subjects from three different datasets. The electrode maps are presented for three different arbitrary frequencies: 2, 10, and 25 Hz in order to show the differences between the three datasets. The power spectrum density pattern shows the distribution of EEG power through the EEG band. In general, the low-frequency spectrum has a higher power density than the high-frequency spectrum. By comparing three different subjects, we can see different amplitudes, electrode maps, and power spectrum density patterns.

TABLE 1. The description of the subjects' characteristics.

	Control	Mild AD	Moderate AD
Number of subjects	35	31	20
Age	66.89 (52-83)	75.23 (63-89)	73.77 (48-87)
Gender (M:F)	16:19	12:19	7:13
Education level (years)	8.77 (2-26)	4.81 (0-11)	4.73 (0-15)
MMSE	28 (20-31)	19.48 (14-24)	14.18 (4-20)
CDR	0	>=0.5 & <=1	2
No. of windows	1426	1514	930
Duration(sec)	11408	12112	7440

2) DATA ACQUISITION SYSTEM

EEG dataset were collected by the Braintech 3.0 instrumentation acquisition system (EMSA Medical equipments

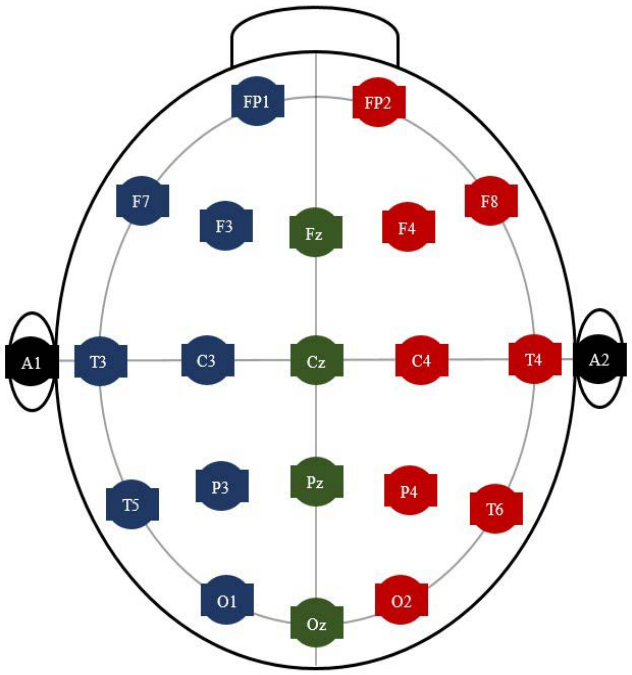

FIGURE 3. Distribution of the EEG acquisition system electrodes on the scalp.

Inc., Brazil) with 12 bits resolution and sampling rate of 200Hz. The electrodes of the EEG data acquisition system were placed according to the International 10–20 System. For this work, the EEG datasets were collected by twenty electrodes Fp1, Fp2, F3, F4, F7, F8, C3, C4, T3, T4, P3, P4, T5, T6, O1, O2, Fz, Cz, Pz, and Oz and two electrodes were placed on the subject's earlobes: A1 and A2 on left and right, respectively. All electrodes were distributed as shown in Figure 3. During the examination, all subjects were awake and relaxed, with closed eyes. Two skilled neurophysiologists manually removed EEG artifacts (e.g., blinking, muscle movements) from the recordings. Subsequently, from each subject, at least 28 epochs of eight seconds were selected by visual inspection [31].

B. PRE-PROCESSING

During the EEG dataset recording, the artifacts, noises and interferences were recorded as well. These artifacts, noises, and interferences were generated from the electrodes, the magnetic fields of the electronic devices, blood pressure, breathing, limb movements, eyes blinking, or other human parties movements [32], [33]. In the preprocessing stage, the EEG signals have been filtered using a band-pass filter to remove the interferences and noises generated during the EEG recording. Different types of finite impulse response (FIR) and infinite impulse response (IIR) filters have been used. In this study, the band pass IIR elliptic digital filter with cutoff frequencies at 0.1 and 60 Hz has been employed. The EEG artifacts (e.g., blinking, muscle movements) were manually removed from the EEG recordings by two skilled neurophysiologists [34].

C. FEATURE EXTRACTION

The feature extraction stage is very important for signal processing, especially EEG signals and other biomedical signals for several reasons: reducing the number of resources of a large dataset without losing any important or relevant information, reducing the dimensionality of a dataset by removing the redundant data, building the model with less machine effort and fewer computations, increasing the speed of learning and training, increasing the accuracy of learned models, reducing the overfitting risk, and improving data visualization. There are several feature extraction techniques used to analyze the EEG signal and decompose the EEG signal into its features. In the present study, we used popular and widespread technique namely Discrete Wavelet Transform (DWT) [35], [36]. DWT is a suitable technique to analyze non-linear and non-stationary signals with different frequencies and different resolutions. DWT analyzes the signal characteristics in the time and frequency domain. DWT decomposes EEG signals into several functions using a single function called the mother function [37] as expressed by.

$$\psi(t) = \frac{1}{\sqrt{2}}\psi\left(\frac{t-y}{x}\right) \quad x, y \in S,\ x > 0 \tag{1}$$

where x and y are the scaling and shifting parameter, respectively, and S is the space of the wavelet. The wavelet transform is shown in the following equation

$$F(x, y) = \frac{1}{\sqrt{x}} \int \psi\left(\frac{t-y}{x}\right) \quad dt \tag{2}$$

In the present work, DWT is employed because the highly efficient representation is provided by DWT represented by Eq. 3. By DWT, EEG filtered signal has been decomposed to high pass and low pass filter to obtain the representation of the signal as an approximation (A1) and detail (D1) coefficients in the first level.

$$F(t) = \sum_{k=-\infty}^{k=+\infty} D_{n,k}\ \ \phi(2^{-n}t - k) + \sum_{k=-\infty}^{k=+\infty}\sum_{k=-\infty}^{k=+\infty} 2^{\frac{-j}{2}} A_{j,k}\psi(2^{-j}t - k) \tag{3}$$

where $A_{j,k}$ and $D_{n,k}$ represent the approximation and detail coefficients, respectively, n is the level, and ψ is the function of scale. In the second level, the approximation coefficients obtained in the first level (A1) will be decomposed into approximation (A2) and detail (D2) coefficients and this process will be repeated again until obtaining the approximation (An) and detail (Dn) coefficients in the last level. At the end of the process, Detail coefficients in each level and approximation coefficients in the last level have been calculated as the EEG signal features. In the present work, the Daubechies 4 (db4) has been employed as a mother wavelet function and four as a decomposition level. Several statistical features have

been investigated to combine with DWT technique in order to construct the feature vectors and to improve the diagnosis system performance. DWT was always combined with a single statistic feature for all subjects in three groups. This process has been repeated with other single statistic feature. Finally, the performance has been compared and evaluated. DWT was not always combined with more than one statistical feature at a time. For a given discrete signal S(n) with mean μ and standard deviation σ, where n = 1, 2, …., N, and N is the number of signal samples, the classical statistical features are not efficient for non-stationary and non-linear signals and usually not a suitable measure for the complex data like EEG signals. We now focus attention on other features and important parameter that describe the data distribution of EEG signals like kurtosis and describe the strength of signals like RMS. It is important to describe the distribution of power and describe the distribution of information for EEG signals like logarithmic band power, average power and norm. those features can be classified easily and accurately using utilized machine learning approaches in our present study. For this reason, we used the following signal features to construct the feature vectors:

1) Logarithmic band power (LBP)

$$LBP = \log(\frac{1}{N}\sum_{n=1}^{N}|S(n)|^2) \tag{4}$$

2) Standard deviation (StD)

$$StD = \sqrt{\frac{1}{N}\sum_{n=1}^{N}(S(n)-\mu)^2} \tag{5}$$

3) Variance (VAR)

$$Var = \frac{1}{N}\sum_{n=1}^{N}(S(n)-\mu)^2 \tag{6}$$

4) Kurtosis (KUR)

$$KUR = \frac{E(S(n)-\mu)^4}{\sigma^4} \tag{7}$$

where E( ) is the expected value of the signal samples.

5) Average Energy (AE)

$$AE = \sum_{n=1}^{N}|S(n)|^2 \tag{8}$$

6) Root mean square (RMS)

$$RMS = \sqrt{\frac{\sum_{n=1}^{N}|S(n)|^2}{N}} \tag{9}$$

7) NO (Norm)

$$NO = \sqrt{\sum_{n=1}^{N}|S(n)|^2} \tag{10}$$

Finally, it is important to present the number of feature vectors that are extracted in the feature extraction stages for three different datasets:

1) Control: 1426 vectors
2) Mild AD: 1514 vectors
3) Moderate AD: 930 vectors

D. CLASSIFICATION AND CROSS-VALIDATION

The diagnosis system can be evaluated in terms of the accuracy of the classifiers, computing the area under the receiver operating characteristic (ROC) curve, sensitivity, and specificity. Several classifiers have been used and evaluated in order to obtain optimal classification accuracy and diagnosis performance. In this study, linear discrimination analysis (LDA), Quadratic discrimination analysis (QDA), support vector machine (SVM), Naïve Bayes (NB), K- nearest neighbor (KNN), Decision tree (DT), Extreme learning machine (ELM), artificial neural network (ANN) and random forest (RF) have been employed.

The operating parameters of the machine learning approaches used in the classification have been carefully chosen. However, the critical parameter for the machine learning approaches is the learning rate parameter. the machine learning approaches are going to skip optimal performance when the learning rate is too fast and If it is too slow, the machine learning approaches may never converge because it is trying really hard to find the optimal performance exactly. As a result, the learning rate parameter for proposed machine learning approaches has been set to 10^{-3}.

In the classification technique, the k-fold cross-validation algorithm has been used, all EEG features are randomly grouped into k equal subsets [38]. One subset is selected for the testing process (for validation), while the remaining subsets are applied for the training process. This procedure has been repeated k times (k-fold), where each subset is used once for the testing process.

In this present work, we used 10-fold cross-validation, where all the EEG signal features have been loaded from the feature matrix that was extracted by the feature extraction techniques and transmitted to the 10-fold cross-validation. Next, these features were divided into a 90% of subset for the training process and a 10% of subset for the testing process. Each time, the training subset was used for training the classifier in order to generate and save the configuration of the trained classifier and the testing subset was transmitted into the trained classifier. Then, the result of the testing classifier will be compared with the state of the original test features for validation and the classifier accuracy will be computed by the following equation.

$$Accuracy = \frac{F_{correct}}{F_{total}} * 100 \tag{11}$$

where $F_{correct}$ is the number of features classified correctly in k iteration, F_{total} is the total number of features to be classified.

TABLE 2. Classification accuracy for Control vs mild AD features based on DWT technique.

Feature Extraction	LDA	QDA	SVM	NB	KNN	DT	ELM	ANN	RF
DWT+LBP	**95.1±0.5**	**99.9±0.1**	**99.8±0.2**	**81.4±0.5**	**99.98±0.02**	97.1±0.2	**99.85±0.05**	90.2±0.3	99.7±0.1
DWT+StD	93.6±0.3	98.2±0.4	99.6±0.1	80.6±0.4	99.96±0.02	96.8±0.3	91.0±0.3	83.8±0.8	99.7±0.1
DWT+VAR	88.0±0.5	82.3±0.5	94.5±0.2	81.3±0.3	99.9±0.04	97.4±0.4	94.7±0.6	62.6±0.5	99.6±0.1
DWT+KUR	73.0±0.4	70.3±0.2	57.2±0.4	75.4±0.6	97.5±0.5	72.1±0.5	58.0±1	78.1±0.4	79.0±0.5
DWT+AE	87.9±0.4	82.3±0.6	95.1±0.5	81.3±0.4	99.92±0.03	96.0±0.3	74.2±0.4	90.8±1	**99.8±0.1**
DWT+RMS	93.6±0.4	98.2±0.3	99.5±0.2	81.0±0.4	**99.98±0.02**	96.8±0.2	90.4±0.4	86.6±0.8	99.7±0.1
DWT+NO	93.4±0.3	97.8±0.3	**99.8±0.2**	81.1±0.5	**99.98±0.02**	**97.5±0.4**	92.5±0.3	**99.7±0.2**	99.7±0.1

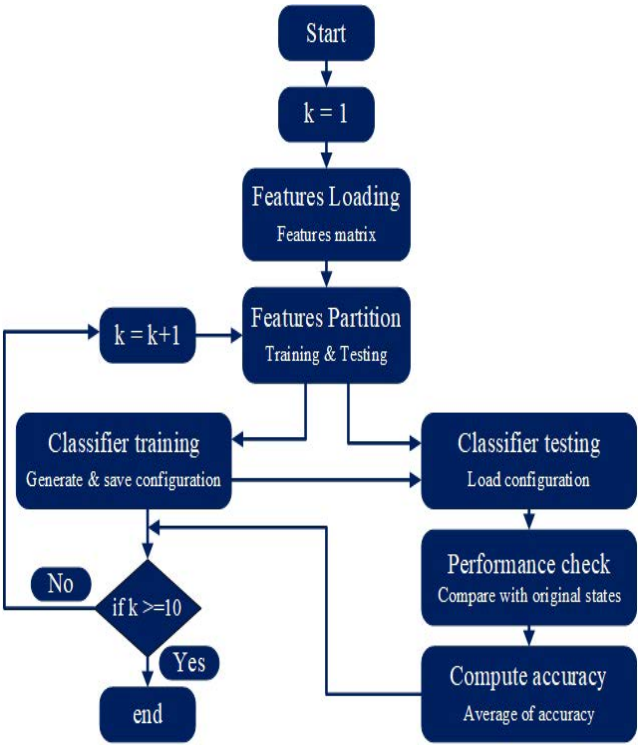

FIGURE 4. Flowchart of 10-fold cross-validation methodology.

This process was repeated ten times; each time, one subset was transmitted into the testing classifier. Finally, the results were averaged to produce a single overall classification accuracy. Figure 4 shows the flowchart of the 10-fold cross-validation methodology.

III. RESULTS AND DISCUSSION

As mentioned before, the EEG datasets utilized in this study have been divided into three groups. The EEG datasets were recorded from 35 Control subjects, 31 mild AD patients, and 20 moderate AD patients in the first, second, and third group, respectively. The EEG datasets have been filtered by a band-pass IIR elliptic digital filter at cut-off frequencies of 0 and 60 Hz for removing the noises and interferences in order to improve the signal-to-noise ratio. Next, the filtered signal has been applied as an input to the DWT technique to extract the features of the EEG filtered signal. Then, the DWT technique has been combined with several statistical features such as LBP, StD, Var, …, etc in order to construct the EEG feature vectors and improve the diagnosis performance. Finally, several types of classifiers have been employed to discriminate the EEG features corresponding to their classes and the classification accuracies have been computed and compared with each other. For more evaluation of the proposed approaches, the receiver operating characteristic curves have been plotted and the areas under these curves have been computed.

According to the number of EEG dataset group, five classification problems have been investigated as following:

1) Control vs mild AD features (2-class)
2) Control vs moderate AD features (2-class)
3) Mild AD vs moderate AD features (2-class)
4) Control vs mild and moderate AD features (2-class)
5) Control vs mild AD vs moderate AD features (3-class)

The classification results for the five classification problems have been presented in section III-A to section III-E.

A. CONTROL VS MILD AD FEATURES (2-CLASS)

In this section, the group of 35 Control subjects forms the class "Control" has been combined with the group of the EEG features extracted from the 31 mild AD patients forms the class "mild AD", resulting the first classification problem (Control vs mild AD). Table 2 presents the overall average classification accuracy of nine classifiers for the first classification problem based on the DWT technique with different combinations of statistical features.

From Table 2, it can be seen that the best classification accuracy has been obtained by ANN, SVM, RF, ELM, QDA, and KNN classifiers achieve to an average accuracy of 99.7, 99.8, 99.8, 99.85, 99.9and 99.98% respectively and the features extracted by DWT+LBP, DWT+AE, and DWT+NO provide the highest classification accuracy. For more evaluation of the proposed approaches, the ROC curves have been plotted in Figure 5. The sensitivity, specificity, classification accuracy, and the area under ROC curves have been computed as shown in Table 3 for all classifiers based on the features provide the best accuracy. The confusion matrices have been presented for all classifiers based on the features provide the best accuracy as shown in Figure 6. It can be seen that the ANN, SVM, RF, ELM, QDA, and KNN classifiers provided the best performance.

TABLE 3. Classifiers' performance based on the best features: sensitivity, specificity, classification accuracy, and area under the ROC curves for the first classification problem.

Classifier	Best Features	Sensitivity %	Specificity %	Accuracy %	AUROCC %
LDA	LBP	**95.21±0.5**	**95.07±0.4**	**95.1±0.5**	**97.2±0.3**
QDA	LBP	**99.93±0.06**	**99.87±0.1**	**99.9±0.1**	**99.98±0.02**
SVM	LBP and NO	**99.79±0.2**	**99.8±0.15**	**99.8±0.2**	**99.98±0.02**
NB	LBP	**82.67±0.75**	**80.87±0.6**	**81.4±0.5**	**90.2±0.3**
KNN	LBP, RMS and NO	**99.98±0.02**	**99.93±0.04**	**99.98±0.02**	**100**
DT	NO	**97.34±0.5**	**97.68±0.5**	**97.5±0.4**	**98.7±0.2**
ELM	LBP	**99.86±0.1**	**99.87±0.1**	**99.86±0.05**	**99.98±0.02**
ANN	NO	**99.65±0.3**	**99.74±0.2**	**99.7±0.2**	**99.96±0.02**
RF	AE	**99.79±0.2**	**99.8±0.15**	**99.8±0.1**	**99.98±0.02**

When we compare our results in this section with those published in similar past research, we see that our approach yielded higher diagnosis accuracy. Morabito *et al.* [16] achieved a maximum accuracy of 85% by using a convolutional neural network classifier. Using DWT + (LBP, RMS, or NO) and KNN classifiers, we achieved a maximum classification accuracy of 99.98 ± 0.02. Further, we find that our study provides the classification accuracy better than the study of Ieracitano *et al.* [18]. Ieracitano *et al.* [18] achieved a maximum accuracy of 96.24% by combining a continuous wavelet transform with a bispectrum feature for feature extraction and a multi-layer perceptron classifier. Our approaches produced the classification accuracy better than Fiscon *et al.* [21] study. Fiscon *et al.* [21] used Fourier transform and WT feature extraction with J48 classifier to achieve 71.7% maximum classification accuracy. Furthermore, the study of Fraga *et al.* [34] used percentage modulation energy for feature extraction and a support vector machine for classification. This system achieved a maximum classification accuracy of 98.4%.

B. CONTROL VS MODERATE AD FEATURES (2-CLASS)

In this section, the group of 35 Control subjects forms the class "Control" has been combined with the group of the EEG features extracted from the 20 moderate AD patients forms the class "moderate AD", resulting the second classification problem (Control vs moderate AD). Table 4 shows the overall average classification accuracy of nine classifiers

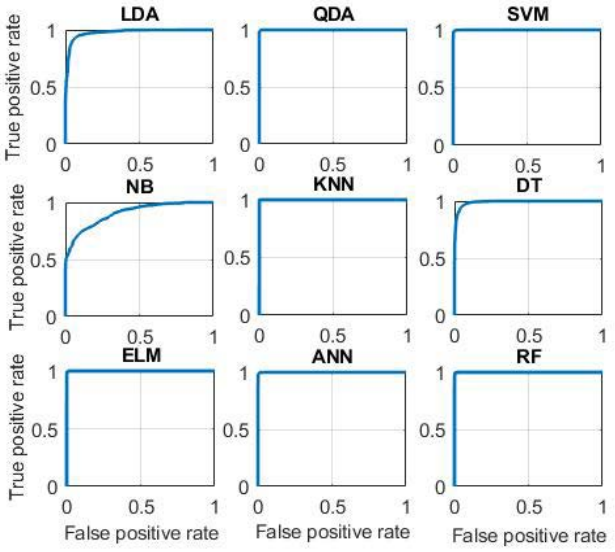

FIGURE 5. ROC curves of all classifiers based on features that provide the best classification accuracy of the first classification problem.

for the second classification problem based on the DWT technique. From Table 4, it can be seen that the features classified by all classifiers provided better results with average classification accuracies between 98.7% and 99.98% except Naïve Bayes classifier with maximum classification accuracy reach to 80.5%.

As seen in Table 4, the features extracted by DWT + LBP, DWT + AE, DWT + RMS, and DWT + NO have the highest classification accuracies. For more evaluation of the proposed approaches, the ROC curves have been plotted in Figure 7. The sensitivity, specificity, classification accuracy, and the area under ROC curves have been computed as shown in Table 5 for all classifiers based on the features provide the best accuracy. The confusion matrices have been presented for all classifiers based on the features that provide the best accuracy as shown in Figure 8. It can be seen that the ANN, SVM, RF, ELM, QDA, and KNN classifiers provided the best performance.

By comparing our results with other studies related to this section, we find that our study achieved an overall classification accuracy reach of 99.98 ± 0.02% higher than the other studies. Morabito *et al.* [16] achieved a maximum accuracy of 85% by using a convolutional neural

TABLE 4. Classification accuracy for Control vs moderate AD features based on DWT technique.

Feature Extraction	LDA	QDA	SVM	NB	KNN	DT	ELM	ANN	RF
DWT+LBP	**98.8±0.3**	**99.98±0.02**	**99.7±0.1**	70.4±0.6	**99.98±0.02**	98.5±0.2	**99.8±0.1**	96.2±0.2	99.7±0.1
DWT+StD	97.9±0.2	99.7±0.3	98.4±0.2	73.9±0.3	99.96±0.02	98.1±0.1	96.9±0.3	92.0±0.3	99.8±0.1
DWT+VAR	92.8±0.3	94.4±0.5	90.6±0.3	73.4±0.4	99.96±0.02	**98.7±0.2**	97.7±0.3	62.6±1.3	99.8±0.1
DWT+KUR	79.8±0.5	83.2±0.5	63.7±0.4	**80.5±0.5**	98.7±0.3	78.1±0.5	59.0±2	87.9±0.4	87.0±0.4
DWT+AE	93.1±0.3	94.2±0.2	90.5±0.3	73.7±0.4	**99.98±0.02**	98.2±0.3	77.4±0.5	97.2±0.3	99.7±0.15
DWT+RMS	97.5±0.2	99.5±0.1	98.4±0.2	74.2±0.5	**98.98±0.02**	98.4±0.2	97.1±0.6	92.8±0.7	99.8±0.1
DWT+NO	97.9±0.3	99.6±0.2	98.6±0.3	74.0±0.5	**99.98±0.02**	98.5±0.3	97.4±0.3	**99.5±0.2**	**99.8±0.1**

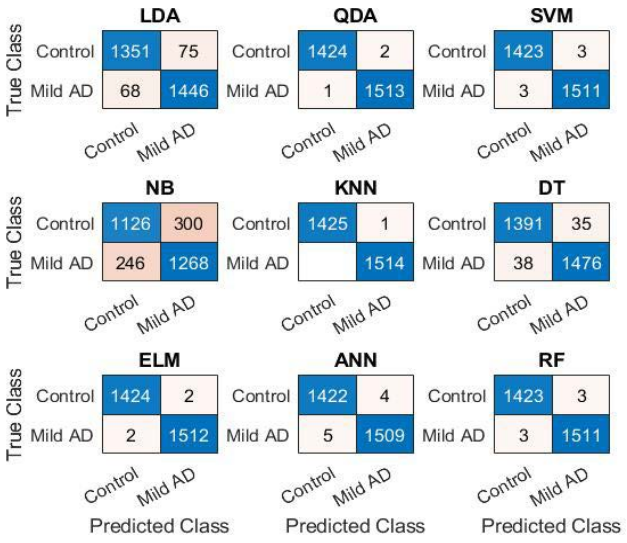

FIGURE 6. Confusion matrices of all classifiers based on features that provide the best classification accuracy of the first classification problem.

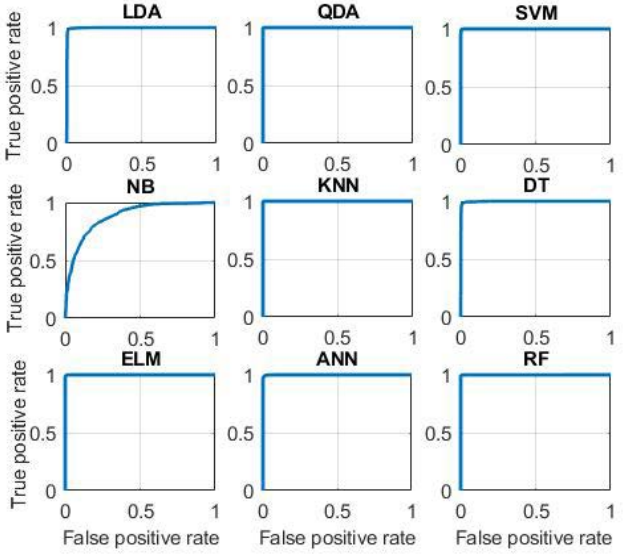

FIGURE 7. ROC curves of all classifiers based on features that provide the best classification accuracy of the second classification problem.

TABLE 5. Classifiers' performance based on the best features: sensitivity, specificity, classification accuracy, and area under the ROC curves for the second classification problem.

Classifier	Best Features	Sensitivity %	Specificity %	Accuracy %	AUROCC %
LDA	LBP	**99.3±0.05**	**98.08±0.2**	**98.8±0.3**	**99.5±0.2**
QDA	LBP	**99.98±0.02**	**99.89±0.06**	**99.98±0.02**	**100**
SVM	LBP	**99.86±0.1**	**99.46±0.1**	**99.7±0.1**	**99.96±0.02**
NB	KUR	**89.79±0.5**	**70.64±0.4**	**80.5±0.5**	**87.2±0.3**
KNN	LBP, AE,RMS and NO	**99.98±0.02**	**99.89±0.07**	**99.98±0.02**	**100**
DT	VAR	**99.15±0.2**	**98.08±0.3**	**98.7±0.2**	**99.4±0.2**
ELM	LBP	**99.86±0.1**	**99.68±0.1**	**99.8±0.1**	**99.98±0.02**
ANN	NO	**99.65±0.3**	**99.25±0.2**	**99.5±0.2**	**99.92±0.02**
RF	NO	**99.86±0.1**	**99.68±0.1**	**99.8±0.1**	**99.98±0.02**

network classifier. Ieracitano *et al.* [18] achieved a maximum accuracy of 96.95% by combining a continuous wavelet transform with a bispectrum feature for feature extraction and a multi-layer perceptron classifier. Bevilacque *et al.* [20] used support vector machines recursive features elimination, principal component analysis, and novel method based on the correlation. Multi-layer perceptron artificial neural network classifier is used to achieve a maximum accuracy reach of 86%. Fiscon *et al.* [21] used Fourier transform and WT feature extraction with J48 classifier to achieve 83%. Triggiani *et al.* [22] used Exact low-resolution brain electromagnetic tomography for feature extraction and an artificial neural network classifier to achieve a maximum diagnosis accuracy of 77%.

C. MILD AD VS MODERATE AD FEATURES (2-CLASS)

In this section, the group of 31 mild AD patients forms the class "mild AD" has been combined with the group of the EEG features extracted from the 20 moderate AD patients forms the class "moderate AD", resulting the third classification problem (mild AD vs moderate AD). Table 6 presents the overall average classification accuracies of nine classifiers for the third classification problem based on the DWT technique. Table 6 includes the average optimal diagnosis performances obtained using SVM, QDA, RF, ANN, and ELM classifiers with the highest classification accuracies of 95.2, 96.4, 97.5, 98.2, and 98.5% respectively. As seen in Table 6, the features extracted by DWT + LBP, DWT + RMS, and DWT + NO provide the highest classification accuracies. For more evaluation of the proposed approaches, the ROC curves have

TABLE 6. Classification accuracy of mild AD vs moderate AD features based on DWT technique.

Feature Extraction	LDA	QDA	SVM	NB	KNN	DT	ELM	ANN	RF
DWT+LBP	**91.1±0.4**	**96.4±0.2**	**95.2±0.3**	69.4±0.5	**94.7±0.3**	94.1±0.4	**98.5±0.2**	87.9±0.4	96.9±0.4
DWT+StD	88.9±0.3	96.3±0.3	93.8±0.4	73.1±0.4	92.2±0.3	93.7±0.3	95.4±0.3	87.6±0.6	97.0±0.4
DWT+VAR	85.8±0.4	89.3±0.6	87.5±0.2	75.8±0.4	92.2±0.4	**94.9±0.4**	90.6±0.5	64.6±0.8	97.0±0.4
DWT+KUR	74.8±0.7	84.2±0.6	65.1±0.3	**78.2±0.5**	94.4±0.4	75.5±0.3	61.0±2.5	83.1±0.4	83.2±0.5
DWT+AE	85.9±0.4	89.3±0.5	87.7±0.5	75.5±0.5	92.3±0.5	94.5±0.5	79.8±0.6	92.0±0.7	96.9±0.3
DWT+RMS	89.0±0.5	**96.4±0.2**	93.9±0.4	72.9±0.4	92.3±0.3	93.8±0.3	94.9±0.4	83.2±0.6	**97.5±0.4**
DWT+NO	88.8±0.4	96.3±0.4	93.8±0.5	73.4±0.6	92.5±0.4	94.2±0.4	95.8±0.3	**98.2±0.5**	97.1±0.5

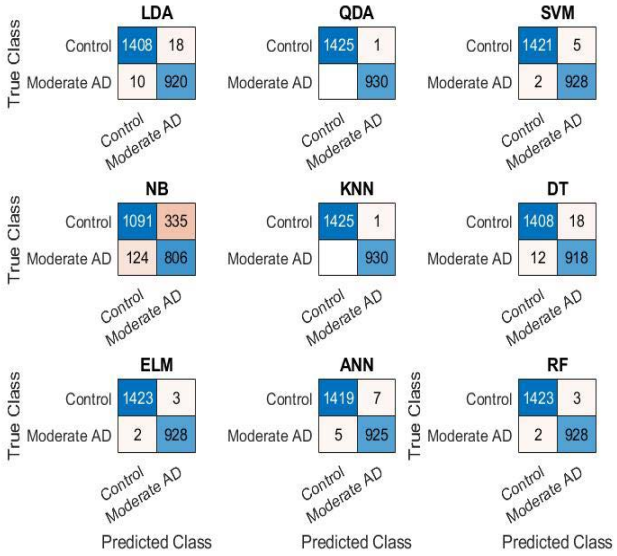

FIGURE 8. Confusion matrices of all classifiers based on features that provide the best classification accuracy of the second classification problem.

TABLE 7. Classifiers' performance based on the best features: sensitivity, specificity, classification accuracy and area under the ROC curves of the third classification problem.

Classifier	Best Features	Sensitivity %	Specificity %	Accuracy %	AUROCC %
LDA	LBP	**93.7±0.6**	**87.2±0.5**	**91.1±0.4**	**96.5±0.3**
QDA	LBP	**99.3±0.7**	**92.2±1.0**	**96.4±0.2**	**98.3±0.1**
SVM	LBP	**97.7±0.8**	**91.5±0.5**	**95.2±0.3**	**97.8±0.2**
NB	KUR	**88.7±3.0**	**67.0±2.0**	**78.2±0.5**	**82.6±0.4**
KNN	LBP	**95.7±0.6**	**93.2±0.5**	**94.7±0.3**	**97.3±0.2**
DT	VAR	**95.9±0.5**	**93.2±0.4**	**94.9±0.4**	**97.4±0.2**
ELM	LBP	**99.4±0.5**	**97.2±0.5**	**98.5±0.2**	**99.3±0.2**
ANN	NO	**99.1±0.7**	**96.9±1.0**	**98.2±0.5**	**99.1±0.3**
RF	RMS	**98.7±0.7**	**95.6±0.6**	**97.5±0.4**	**98.7±0.2**

been plotted as shown in Figure 9. The sensitivity, specificity, classification accuracy, and the area under ROC curves have been computed as shown in Table 7 for all classifiers based on the features provide the best accuracy. The confusion matrices have been presented for all classifiers based on the features that provide the best accuracy as shown in Figure 10. It can be seen that the SVM, QDA, RF, ANN, and ELM classifiers provided the best performance.

By comparing our results in this section with other studies, we find that our work provided the overall classification accuracy reach of 98.5 ± 0.2% higher than those reported in other studies. Morabito *et al.* [16] achieved a maximum accuracy of 78% by using a convolutional neural network classifier. Ieracitano *et al.* [18] achieved a maximum accuracy of 90.24% by combining a continuous wavelet transform with a bispectrum feature for feature extraction and a multi-layer perceptron classifier. Fiscon *et al.* [21] used Fourier transform and WT feature extraction with J48 classifier to achieve classification accuracy up to 80.2%. Amezquita-Sanchez *et al.* [23] used multiple signal classification and empirical wavelet transform, different nonlinear

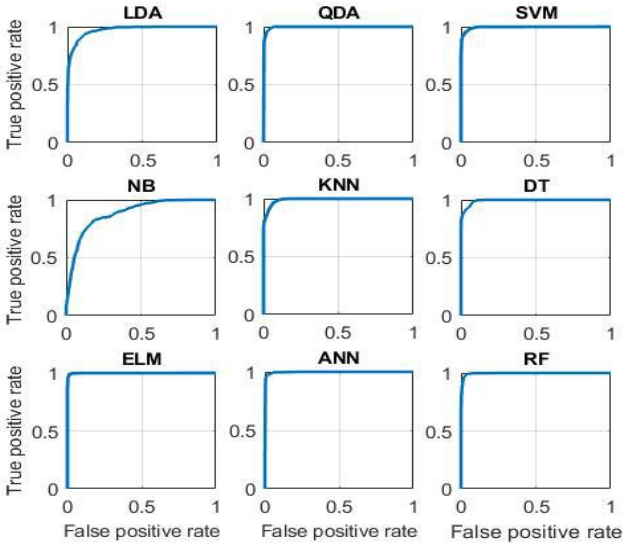

FIGURE 9. ROC curves of all classifiers based on features that provide the best classification accuracy of the third classification problem.

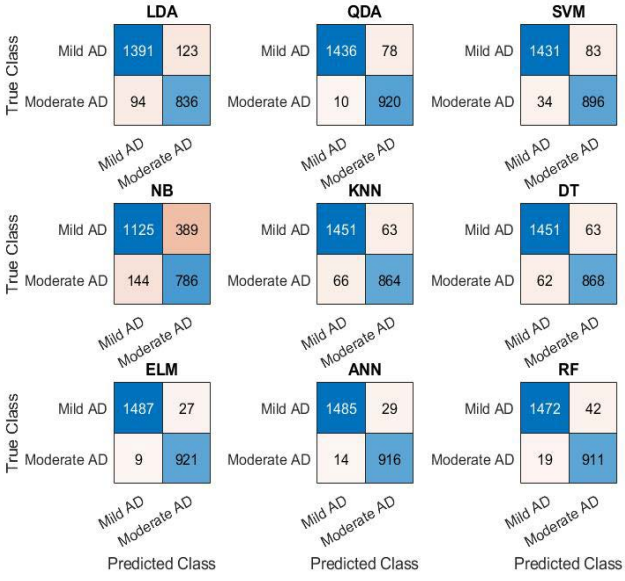

FIGURE 10. Confusion matrices of all classifiers based on features that provide the best classification accuracy of the third classification problem.

features such as fractality dimension from the chaos theory, and enhanced probabilistic neural network model. The proposed approach achieved a maximum diagnosis accuracy of 90.3%. Fraga *et al.* [34] used percentage modulation energy for feature extraction and support vector machine for classification. This system achieved diagnosis accuracy reach to 94%.

D. CONTROL VS MILD AND MODERATE AD FEATURES (2-CLASS)

In this section, the group of 35 Control subjects forms the class "Control" has been combined with the group of the EEG features extracted from both of two groups of

TABLE 8. Classification accuracy of control vs mild and moderate AD features based on DWT technique.

Feature Extraction	LDA	QDA	SVM	NB	KNN	DT	ELM	ANN	RF
DWT+LBP	**93.3±0.3**	**99.9±0.04**	**99.2±0.3**	**77.2±0.5**	**99.98±0.02**	**97.8±0.3**	**99.6±0.3**	96.4±0.5	99.5±0.2
DWT+StD	91.4±0.5	91.3±0.2	98.4±0.3	76.5±0.4	99.96±0.02	97.5±0.4	86.9±0.5	83.9±0.4	**99.8±0.1**
DWT+VAR	84.8±0.5	81.2±0.4	92.3±0.4	74.8±0.5	99.87±0.05	97.5±0.4	90.6±0.4	65.4±2	99.6±0.1
DWT+KUR	75.9±0.4	63.8±0.5	64.6±0.7	74.6±0.3	97.9±0.2	72.1±0.7	63.0±2	79.5±0.4	78.6±0.5
DWT+AE	84.5±0.6	81.4±0.6	92.2±0.3	75.1±0.4	**99.98±0.02**	**97.8±0.3**	71.9±0.6	92.3±1	**99.8±0.1**
DWT+RMS	91.2±0.3	91.2±0.3	98.5±0.4	77.1±0.3	**99.98±0.02**	**97.8±0.3**	87.0±0.4	85.3±0.6	**99.8±0.1**
DWT+NO	91.3±0.5	91.8±0.6	98.6±0.5	76.9±0.4	**99.98±0.02**	97.4±0.3	89.9±0.4	**99.7±0.1**	99.6±0.1

TABLE 9. Classifiers' performance based on the best features: sensitivity, specificity, accuracy, and area under the ROC curves of the fourth classification problem.

Classifier	Best Features	Sensitivity. %	Specificity %	Accuracy %	AUROCC%
LDA	LBP	**95.02±0.5**	**90.5±0.5**	**93.3±0.3**	**95.4±0.2**
QDA	LBP	**99.96±0.02**	**99.86±0.04**	**99.9±0.04**	**99.98±0.02**
SVM	LBP	**99.4±0.4**	**98.9±0.3**	**99.2±0.3**	**99.86±0.02**
NB	LBP	**78.4±0.8**	**74.1±1.0**	**77.2±0.5**	**81.4±0.3**
KNN	LBP, AE, RMS and NO	**99.96±0.02**	**99.98±0.02**	**99.98±0.02**	**100**
DT	LBP, AE and RMS	**98.05±0.5**	**97.5±0.4**	**97.8±0.3**	**99.2±0.2**
ELM	LBP	**99.7±0.3**	**99.4±0.2**	**99.6±0.3**	**99.94±0.02**
ANN	NO	**99.8±0.1**	**99.6±0.2**	**99.8±0.1**	**99.58±0.2**
RF	StD, AE and RMS	**99.9±0.04**	**99.7±0.1**	**99.8±0.1**	**99.8±0.15**

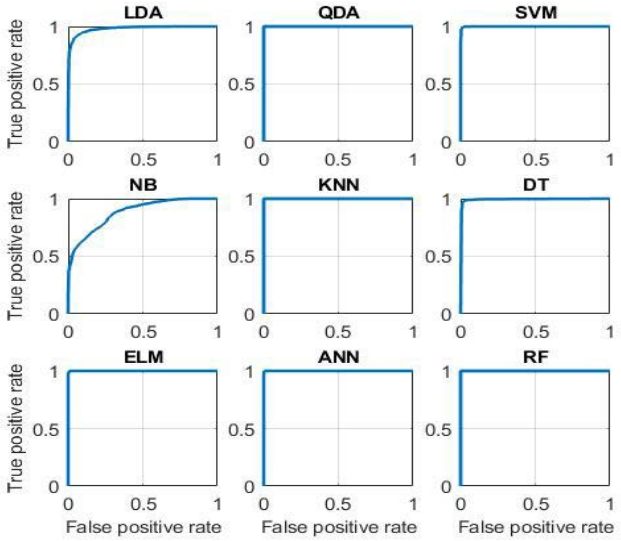

FIGURE 11. ROC curves of all classifiers based on features that provide the best classification accuracy of the fourth classification problem.

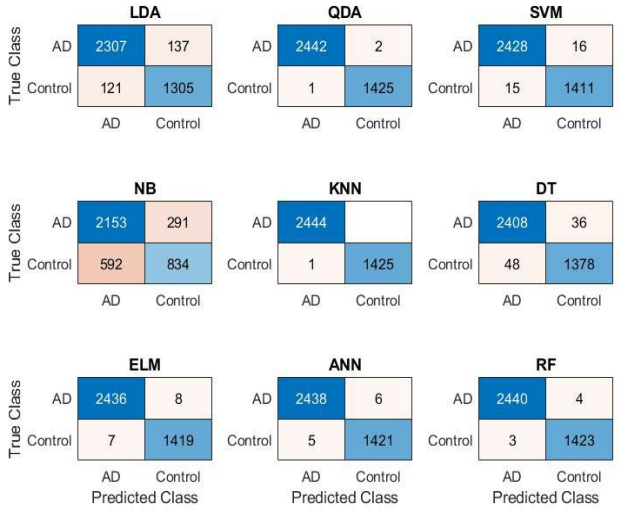

FIGURE 12. Confusion matrices of all classifiers based on features that provide the best classification accuracy of the fourth classification problem.

the 31 mild AD and 20 moderate AD patients forms the class ''mild & moderate AD'', resulting the fourth classification problem (Control vs mild & moderate AD). Table 8 shows the classification accuracy of nine classifiers for the forth classification problem based on the DWT technique. From Table 8, it can be seen that the features classified by all classifiers provided better results with average classification accuracies between 97.8 and 99.98% except LDA and NB classifiers with average classification accuracies of 93.3 and 77.2% respectively. As seen in Table 8, the features extracted by DWT + LBP, DWT + AE, DWT + RMS, and DWT + NO provide the highest classification accuracies. For more evaluation of the proposed approaches, the ROC curves have been plotted as shown in Figure 11. The sensitivity, specificity, classification accuracy, and the area under ROC curves have been computed as shown in Table 9 for all classifiers based on the features that provide the best accuracy. The confusion matrices have been presented for all classifiers based on the features that provide the best accuracy as shown in Figure 12. It can be seen that all classifiers provided the best performance except LDA and NB. By comparing our results in this section with other studies, we find that our work provided the overall classification accuracy reach of 99.98 ± 0.02% higher than those reported in other studies. Cassani *et al.* [17] used an automated artifact removal algorithm with common EEG features, spectral power, and coherence to extract the amplitude-modulation features and support vector machine for classification to achieve a maximum accuracy of 91.1%. Trambaiolli *et al.* [19] used Wavelet and visibility graph for feature extraction with support vector machine classifier

TABLE 10. Classification accuracy of Control vs mild AD vs moderate AD features based on DWT technique.

Feature Extraction	LDA	QDA	SVM	NB	KNN	DT	ELM	ANN	RF
DWT+LBP	**88.0±0.4**	**98.1±0.5**	**96.5±0.3**	58.5±1.5	**96.7±0.4**	93.5±0.2	**98.1±0.5**	71.6±0.5	97.5±0.2
DWT+StD	85.7±0.4	95.9±0.5	93.7±0.4	61.0±0.8	95.5±0.4	93.3±0.5	86.9±0.5	85.2±0.3	96.7±0.1
DWT+VAR	74.7±0.3	79.4±0.3	90.6±0.3	64.4±0.5	95.3±0.5	93.8±0.5	87.1±0.3	52.1±0.7	97.2±0.3
DWT+KUR	62.9±0.6	64.4±0.4	52.7±0.5	**67.7±0.6**	95.9±0.4	60.3±0.4	56.1±0.5	67.8±0.6	76.8±0.6
DWT+AE	75.8±0.4	79.4±0.5	90.6±0.4	64.8±0.5	95.0±0.3	**94.3±0.4**	65.4±0.4	87.1±0.5	**97.7±0.3**
DWT+RMS	85.8±0.4	96.1±0.5	93.6±0.3	61.1±0.6	95.3±0.3	93.9±0.3	85.2±0.5	74.3±0.5	97.2±0.2
DWT+NO	85.8±0.5	96.0±0.5	93.7±0.5	61.7±0.5	95.5±0.4	94.1±0.4	88.6±0.4	**97.5±0.6**	97.4±0.2

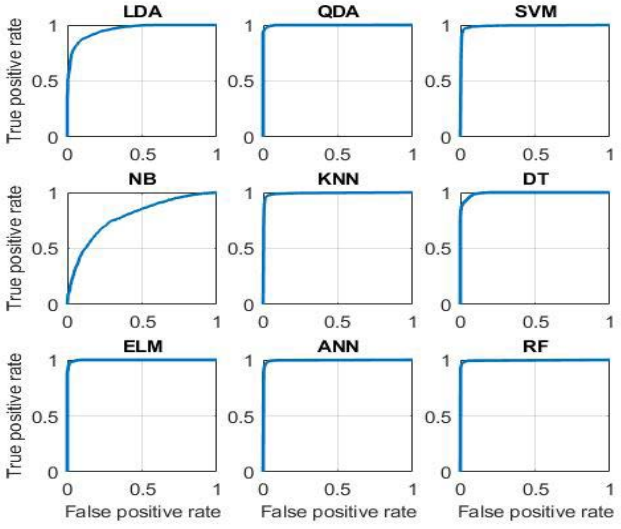

FIGURE 13. ROC curves of all classifiers based on features that provide the best classification accuracy of the fifth classification problem.

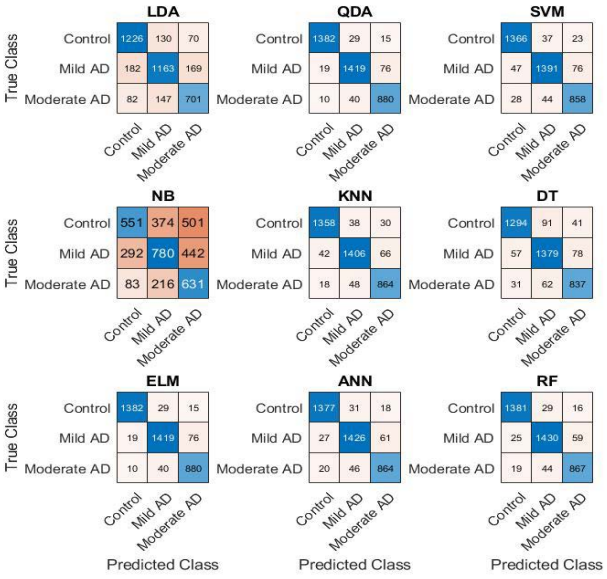

FIGURE 14. Confusion matrices of all classifiers based on features that provide the best classification accuracy of the fifth classification problem.

is achieve classification accuracy up to 91.81%. Fiscon *et al.* [21] used Fourier transform and WT feature extraction with J48 classifier to achieve classification accuracy up to 80.2%. Kanda *et al.* [30] used a morlet wavelet filter for feature extraction with a support vector machine technique for classification to produce a classification accuracy up to 92.72%. Cassani *et al.* [31] computed three EEG signal features: spectral, coherence, and amplitude modulation and then used a support vector machine for classification to achieve a maximum accuracy reach of 84.7%. Furthermore, the study of Fraga *et al.* [34] used percentage modulation energy for feature extraction and support vector machine for classification. This system achieved a maximum classification accuracy of 98.4%.

E. CONTROL VS MILD AD VS MODERATE AD FEATURES (3-CLASS)

In this section, the group of 35 Control subjects forms the first class ''Control'', has been combined with the group of the EEG features extracted from the group of the 31 mild AD patients forms the second class ''mild AD'' and combined with the group of the EEG features extracted from the group of the 20 moderate AD patients forms the third class ''moderate AD'', resulting the fifth classification problem (Control vs mild AD vs moderate AD). Table 10 shows

TABLE 11. Classifiers' performance based on the best features:sensitivity, specificity, classification accuracy, and area under the ROC curves of the fifth classification problem.

Classifier	Best Features	Sensitivity %	Specificity %	Accuracy %	AUROCC %
LDA	LBP	**82.3±0.5**	**91.6±0.7**	**88.0±0.4**	**94.0±0.3**
QDA	LBP	**97.9±0.4**	**98.2±0.5**	**98.1±0.5**	**99.3±0.3**
SVM	LBP	**94.8±0.6**	**97.5±1.0**	**96.5±0.3**	**98.4±0.2**
NB	KUR	**59.5±3.0**	**70.3±3.0**	**67.7±0.8**	**73.6±0.7**
KNN	LBP	**95.8±0.4**	**97.2±0.5**	**96.7±0.5**	**98.8±0.2**
DT	AE	**93.6±0.6**	**94.7±0.6**	**94.3±0.4**	**96.5±0.3**
ELM	LBP	**97.9±0.5**	**98.2±0.4**	**98.1±0.5**	**99.3±0.3**
ANN	NO	**96.7±0.3**	**98.0±0.3**	**97.5±0.6**	**98.6±0.4**
RF	AE	**96.9±0.3**	**98.2±0.4**	**97.7±0.3**	**98.9±0.2**

the classification accuracy of nine classifiers for the fifth classification problem based on the DWT technique. From Table 10, it can be seen that the features classified by SVM, KNN, ANN, RF, QDA, and ELM provided better results with average classification accuracies of 96.5, 96.7, 97.5, 97.7, 98.1, and 98.1%, respectively.

As seen in Table 10, the features extracted by DWT + LBP, DWT + AE, and DWT + NO provide the highest classification accuracies. For more evaluation of the proposed

TABLE 12. Comparison of the classification results for Alzheimer's disease diagnosis.

The authors	Pre-processing	Feature Extraction	Classification	Problem	Dataset	Accuracy %
Morabito et al [16]	———-	———-	CNN	AD vs MCI	Italian	78
				CS vs AD		85
				CS vs MCI		85
				CS vs MCI vs AD		82
Cassani et al. [17]	wICA	spectral power, coherence and amplitude-modulation features	SVM	CS vs (Mild, Moderate and Severe AD)	US & Brazilian	91.4
Ieracitano et al. [18]	Manually	CWT and BiS	MLP, LR, SVM	CS vs MCI	Italian	96.24
				CS vs AD		96.95
				MCI vs AD		90.24
				CS vs MCI vs AD		89.22
Trambaiolli et al. [19]	Manually	Wavelet and visibility graph	SVM	CS vs (Mild and Moderate AD)	Brazilian	76.88
Bevilacque et al. [20]	———-	SVMR FE,PCA	SVM, MLP-ANN	CS vs AD	Spanish	86
Fiscon e al [21]	———-	FT ,wavelet	J48	CS vs MCI	Italian	71.7
				CS vs AD		72.2
				MCI vs AD		80.2
				CS vs (MCI and AD)		74.7
Triggiani et al. [22]	Manually	eLORETA	ANN	CS vs AD	Italian	76.7
Amezquita-Sanchez et al. [23]	Manually	MUSIC-EWT with fractality dimension	EPNN	MCI vs AD	Italian	90.3
Kanda et al. [30]	——-	Morlet wavelet filter	SVM	CS vs (Mild and Moderate AD)	Brazilian	83.95
Cassani et al. [31]	wICA	Spectral, Coherence, and Amplitude modulation	SVM	CS vs (Mild, Moderate and Severe AD)	Brazilian	84.7
Fraga et al. [34]	Manually	percentage modulation energy	SVM	CS vs Mild AD	Brazilian	98.4
				Mild vs Moderate AD		94
				CS vs (Mild AD + Moderate AD)		98.4
Our work	Manually	**DWT + LBP, StD, VAR, KUR, AE, RMS and NO**	**LDA, QDA, SVM, NB, KNN, DT, ELM, ANN, RF**	**CS vs Mild AD**	**Brazilian**	**99.98**
				CS vs Moderate AD		**99.98**
				Mild vs Moderate AD		**98.5**
				CS vs (Mild + Moderate AD)		**99.98**
				CS vs Mild AD vs Moderate AD		**98.1**

TABLE 13. Summary of the best results for Alzheimer's disease diagnosing methods of five classification problems.

CP	Best Features	Classifier	Sensitivity %	Specificity %	Accuracy %	AUROCC %
I	LBP RMS NO	KNN	**99.98±0.02**	**99.93±0.04**	**99.98±0.02**	**100**
II	LBP AE RMS NO	KNN	**99.98±0.02**	**99.89±0.06**	**99.98±0.02**	**100**
III	LBP	ELM	**99.4±0.5**	**97.2±0.5**	**98.5±0.2**	**99.3±0.2**
IV	LBP AE RMS NO	KNN	**99.96±0.02**	**99.98±0.02**	**99.98±0.02**	**100**
V	LBP	QDA ELM	**97.9±0.5**	**98.2±0.4**	**98.1±0.5**	**99.3±0.3**

approaches, the ROC curves have been plotted in Figure 13. The sensitivity, specificity, classification accuracy, and the area under ROC curves have been computed as shown in Table 11 for all classifiers based on the features that provide the best accuracy. The confusion matrices have been presented for all classifiers based on the features that provide the best accuracy as shown in Figure 14. It can be seen that the SVM, KNN, ANN, RF, QDA, and ELM classifiers provided the best performance. By comparing our results in this section with other studies, we find that our work provided the overall diagnosis accuracy reach of $98.1 \pm 0.5\%$ higher than those reported in other studies. Morabito *et al.* [16] achieved a maximum accuracy of 82% by using a convolutional neural network classifier. Ieracitano *et al.* [18] achieved a maximum accuracy of 89.22% by combining a continuous wavelet transform with a bispectrum feature for feature extraction and a multi-layer perceptron classifier.

The gain of this work can be measured by comparing the results of the proposed method with the results of the previous studies. Table 12 shows the comparison of our work results with the results of the previous works related to Alzheimer's disorder. From Table 12, it can be seen that our work provides a higher classification accuracy better than the previous studies.

Finally, we know that the human brain is the most complicated element of the human body and that it contains a wealth of information about neurological disorders. Furthermore, we know that the majority of neurological brain disorders diagnoses are performed manually by neurologists or competent clinicians by visual analysis of EEG patterns. As a result, in this work, we developed a computer-aided diagnosis system capable of automatically analyzing EEG Alzheimer's disorder signals and providing early diagnosis for Alzheimer's disease. By evaluating the proposed system, the results in two-class or three-class diagnosis indicate superior performance and greater accuracies than similar prior studies reported in the literature. The suggested system can help medical physicians and clinicians for early diagnosis of Alzheimer's disease automatically, quickly, easily, effectively, and precisely. As a result of the suggested method, the restricted number of neurologists may be decreased, diagnostic time saved, and diagnosis accuracy raised.

Although the machine-learning systems bring huge benefits to the health sector, machine learning systems have some drawbacks. The bigger problem with machine learning approaches-related is errors and injuries. Machine-learning approaches are prone to errors, which eventually lead to patient injury or other significant problems. For instance, a patient may take a drug wrongly recommended by the machine learning approaches, leading to more questions. The second drawback of machine learning systems is inequality and Discrimination. The machine learning systems are not immune to bias. In fact, the faintest hint of discrimination is always reflected in the results. For instance, when data sourced from academic medical centers is fed into machine learning systems, such a system may struggle to treat or benefit populations from other areas apart from academic medical centers. The efficiency of the machine learning system may reduce when the provider is of gender or race which is a minority in the training data. In the health sector, the machine learning approaches need huge, curate accurate, high-quality medical data and should be available for researchers but the strict confidentiality and privacy laws guarding medical records worldwide make the machine learning approaches with small datasets questionable and this is one of the machine learning systems drawbacks.

Although the fact that we presented the usefulness of our proposal approaches, some limitations need to be addressed. The utilized EEG clinical dataset is not relatively big because it consisting of 35 control subjects, 31 Mild AD subjects, and 22 moderate AD subjects. A larger, public dataset could validate the robustness of the proposed method and further demonstrate the generality of the method for EEG signals classification. So, the validation of this experiment with a larger dataset and the extension of this methodology so that the input signals that can be taken from a variety of EEG recorders are of great importance and will be taking place in future work. Moreover, taking into account the severe AD, it would be useful to characterize different subtypes of AD disease and evaluate our system by different types of AD disease including severe AD and more analysis the characterize subjects with mild AD, those who progress to moderate AD and those who progress to severe AD. Finally, only one feature extraction approach (DWT) has been used in this study and machine learning approaches have been used for classification. In future research works, the usefulness of other advanced feature extraction approaches and deep learning classification methods should be investigated. The

proposed diagnosis system will be evaluated using different neurological brain disorders and implemented as a hardware system for real-time diagnosis.

IV. CONCLUSION

In this present study, we focused on the development of a diagnosis system for Alzheimer's disease using EEG signals analysis. The development of an Alzheimer's diseases diagnosis system which is able to automatically analyze brain signals will improve the diagnosis speed as well as the accuracy of the diagnosis process. In this present work, the recorded EEG datasets have been filtered by band-pass filter. Next, the DWT technique has been investigated to decompose the filtered signal to its frequency bands and several signal features have been combined with the DWT technique in order to improve the diagnosis performance. After that, nine machine learning techniques have been investigated to classify EEG features to their corresponding classes. These investigations aim to compare the proposed approaches and recommend the best combination method for the diagnosis of Alzheimer diseases.

The utilized datasets have been divided into three groups: Control, mild AD, and moderate AD group. From these groups, five classification problems have been investigated: Control vs mild AD group, Control vs moderate AD group, mild vs moderate AD group, Control vs mild and moderate AD group, and Control vs mild AD vs moderate AD group. The proposed diagnosis system has been evaluated by those five classification problems. The proposed system achieved an average classification accuracy reach of 99.98% and AUROCC reach of 100% with DWT + (LBP, RMS or NO) + KNN combinations in the first, second and fourth problems. In the third problem, the proposed system achieved an average classification accuracy reach of 98.5% and AUROCC reach of 99.3% with DWT + LBP + ELM combination. In the fifth problem, the proposed system achieved an average classification accuracy reach of 98.1% and AUROCC reach of 99.3% with DWT + LBP + (QDA or ELM) combinations. Table 13 shows the summary of the best results for Alzheimer's disease diagnosing methods of five classification problems. From Table 13, it can be seen the best combination is DWT + (LBP, AE, RMS, and NO) + KNN for Alzheimer's disease stages detection from the control group (Classification problems I, II, and IV) or ELM for Alzheimer's disease stages detection from each other (Classification problems III and V)).

REFERENCES

[1] A. Caruso, F. Nicoletti, D. Mango, A. Saidi, R. Orlando, and S. Scaccianoce, "Stress as risk factor for Alzheimer's disease," *Pharmacol. Res.*, vol. 132, pp. 130–134, Jun. 2018.

[2] H. M. Fonteijn, M. Modat, M. J. Clarkson, and J. Barnes, "An event-based model for disease progression and its application in familial Alzheimer's disease and Huntington's disease," *NeuroImage*, vol. 60, no. 3, pp. 1880–1889, 2012.

[3] A. Ghanemi, "Alzheimer's disease therapies: Selected advances and future perspectives," *Alexandria J. Med.*, vol. 51, no. 1, pp. 1–3, 2015.

[4] A. Burns and S. Iliffe, "Alzheimer's disease," *Bmj*, vol. 338, no. 7692, pp. 467–471, 2009, doi: 10.1136/bmj.b158.

[5] *Neurological Disorders: Public Health Challenges*. World Health Organization, Geneva, Switzerland, 2006.

[6] *Dementia Fact Sheet World Health Organization*, World Health Organization, Geneva, Switzerland, 2018.

[7] R. Lipton, T. J. Schwedt, and B. W. Friedman, "Global, regional, and national incidence, prevalence, and years lived with disability for 310 diseases and injuries, 1990–2015: A systematic analysis for the Global Burden of disease study 2015," *Lancet*, vol. 388, no. 10053, pp. 1545–1602, 2016.

[8] R. K. Chikara and L.-W. Ko, "Neural activities classification of human inhibitory control using hierarchical model," *Sensors*, vol. 19, no. 17, p. 3791, Sep. 2019.

[9] L. Ko, R. K. Chikara, Y. Lee, and W. Lin, "Exploration of user's mental state changes during performing brain–computer interface," *Sensors*, vol. 20, no. 11, p. 3169, Jun. 2020.

[10] R. Djemal, K. AlSharabi, S. Ibrahim, and A. Alsuwailem, "EEG-based computer aided diagnosis of autism spectrum disorder using wavelet, entropy, and ANN," *BioMed Res. Int.*, vol. 2017, pp. 1–9, 2017.

[11] K. AlSharabi, S. Ibrahim, R. Djemal, and A. Alsuwailem, "A DWT-entropy-ANN based architecture for epilepsy diagnosis using EEG signals," in *Proc. 2nd Int. Conf. Adv. Technol. Signal Image Process. (ATSIP)*, Mar. 2016, pp. 288–291.

[12] F. A. Alturki, K. AlSharabi, M. Aljalal, and A. M. Abdurraqeeb, "A DWT-band power-SVM based architecture for neurological brain disorders diagnosis using EEG signals," in *Proc. 2nd Int. Conf. Comput. Appl. Inf. Secur. (ICCAIS)*, May 2019, pp. 1–4.

[13] F. A. Alturki, K. AlSharabi, A. M. Abdurraqeeb, and M. Aljalal, "EEG signal analysis for diagnosing neurological disorders using discrete wavelet transform and intelligent techniques," *Sensors*, vol. 20, no. 9, p. 2505, Apr. 2020.

[14] F. A. Alturki, M. Aljalal, A. M. Abdurraqeeb, K. Alsharabi, and A. A. Al-Shamma'a, "Common spatial pattern technique with EEG signals for diagnosis of autism and epilepsy disorders," *IEEE Access*, vol. 9, pp. 24334–24349, 2021.

[15] M. Aljalal, S. A. Aldosari, K. AlSharabi, A. M. Abdurraqeeb, and F. A. Alturki, "Parkinson's disease detection from resting-state EEG signals using common spatial pattern, entropy, and machine learning techniques," *Diagnostics*, vol. 12, no. 5, p. 1033, 2022.

[16] F. C. Morabito, M. Campolo, C. Ieracitano, J. M. Ebadi, L. Bonanno, A. Bramanti, S. Desalvo, N. Mammone, and P. Bramanti, "Deep convolutional neural networks for classification of mild cognitive impaired and Alzheimer's disease patients from scalp EEG recordings," in *Proc. IEEE 2nd Int. Forum Res. Technol. Soc. Ind. Leveraging Better Tomorrow (RTSI)*, Sep. 2016, pp. 1–6.

[17] R. Cassani, T. H. Falk, F. J. Fraga, M. Cecchi, D. K. Moore, and R. Anghinah, "Towards automated electroencephalography-based alzheimer's disease diagnosis using portable low-density devices," *Biomed. Signal Process. Control*, vol. 33, pp. 261–271, 2017.

[18] C. Ieracitano, N. Mammone, A. Hussain, and F. C. Morabito, "A novel multi-modal machine learning based approach for automatic classification of EEG recordings in dementia," *Neural Netw.*, vol. 123, pp. 176–190, Mar. 2020.

[19] L. Trambaiolli, N. Spolaôr, A. Lorena, R. Anghinah, and J. Sato, "Feature selection before EEG classification supports the diagnosis of Alzheimer's disease," *Clin. Neurophysiol.*, vol. 128, no. 10, pp. 2058–2067, 2017.

[20] V. Bevilacqua, A. A. Salatino, C. Di Leo, G. Tattoli, D. Buongiorno, D. Signorile, C. Babiloni, C. Del Percio, A. I. Triggiani, and L. Gesualdo, "Advanced classification of Alzheimer's disease and healthy subjects based on EEG markers," in *Proc. Int. Joint Conf. Neural Netw. (IJCNN)*, Jul. 2015, pp. 1–5.

[21] G. Fiscon, E. Weitschek, A. Cialini, G. Felici, P. Bertolazzi, S. De Salvo, A. Bramanti, P. Bramanti, and M. C. De Cola, "Combining EEG signal processing with supervised methods for Alzheimer's patients classification," *BMC Med. Inform. Decis. Making*, vol. 18, no. 1, pp. 1–10, 2018.

[22] A. I. Triggiani, V. Bevilacqua, A. Brunetti, R. Lizio, G. Tattoli, F. Cassano, A. Soricelli, R. Ferri, F. Nobili, and L. Gesualdo, "Classification of healthy subjects and Alzheimer's disease patients with dementia from cortical sources of resting state EEG rhythms: A study using artificial neural networks," *Frontiers Neurosci.*, vol. 10, p. 604, Jan. 2017.

[23] J. P. Amezquita-Sanchez, N. Mammone, F. C. Morabito, S. Marino, and H. Adeli, "A novel methodology for automated differential diagnosis of mild cognitive impairment and the Alzheimer's disease using EEG signals," *J. Neurosci. Methods*, vol. 322, pp. 88–95, Jul. 2019.

[24] E. Perez-Valero, M. Á. Lopez-Gordo, C. M. Gutiérrez, I. Carrera-Muñoz, and R. M. Vílchez-Carrillo, "A self-driven approach for multi-class discrimination in Alzheimer's disease based on wearable EEG," *Comput. Methods Programs Biomed.*, vol. 220, Jun. 2022, Art. no. 106841.
[25] T. Araújo, J. P. Teixeira, and P. M. Rodrigues, "Smart-data-driven system for Alzheimer disease detection through electroencephalographic signals," *Bioengineering*, vol. 9, no. 4, p. 141, Mar. 2022.
[26] M. Alessandrini, G. Biagetti, P. Crippa, L. Falaschetti, S. Luzzi, and C. Turchetti, "EEG-Based Alzheimer's disease recognition using robust-PCA and LSTM recurrent neural network," *Sensors*, vol. 22, no. 10, p. 3696, 2022.
[27] S. Brucki, R. Nitrini, P. Caramelli, P. Bertolucci, and I. H. Okamoto, "Suggestions for utilization of the mini-mental state examination in Brazil," *Arquivos de Neuro-Psiquiatria*, vol. 61, no. 3B, pp. 777–781, 2003.
[28] G. McKhann, D. Drachman, M. Folstein, R. Katzman, D. Price, and E. M. Stadlan, "Clinical diagnosis of Alzheimer's disease: Report of the NINCDS-ADRDA work group* under the auspices of Department of Health and Human services task force on Alzheimer's disease," *Neurol.*, vol. 34, no. 7, p. 939, 1984.
[29] *Diagnostic and Statistical Manual of Mental Disorders*, American Psychiatric Association, Washington, DC, USA, 1980, vol. 3.
[30] P. A. M. Kanda, L. R. Trambaiolli, A. C. Lorena, F. J. Fraga, L. F. I. Basile, R. Nitrini, and R. Anghinah, "Clinician's road map to wavelet EEG as an Alzheimer's disease biomarker," *Clin. EEG Neurosci.*, vol. 45, no. 2, pp. 104–112, 2014.
[31] R. Cassani, T. H. Falk, F. J. Fraga, P. A. Kanda, and R. Anghinah, "Towards automated EEG-based Alzheimer's disease diagnosis using relevance vector machines," in *Proc. 5th ISSNIP-IEEE Biosignals Biorobot. Conf., Biosignals Robot. Better Safer Living (BRC)*, May 2014, pp. 1–6.
[32] J. Müller-Gerking, G. Pfurtscheller, and H. Flyvbjerg, "Designing optimal spatial filters for single-trial EEG classification in a movement task," *Clin. Neurophysiol.*, vol. 110, no. 5, pp. 787–798, 1999.
[33] X. Perrin, "Semi-autonomous navigation of an assistive robot using low throughput interfaces," Ph.D. dissertation, ETH Zurich, Zürich, Switzerland, 2009.
[34] F. J. Fraga, T. H. Falk, L. R. Trambaiolli, E. F. Oliveira, W. H. L. Pinaya, P. A. M. Kanda, and R. Anghinah, "Towards an EEG-based biomarker for Alzheimer's disease: Improving amplitude modulation analysis features," in *Proc. IEEE Int. Conf. Acoust., Speech Signal Process.*, May 2013, pp. 1207–1211.
[35] B. K. Panigrahi, P. K. Ray, P. K. Rout, A. Mohanty, and K. Pal, "Detection and classification of faults in a microgrid using wavelet neural network," *J. Inf. Optim. Sci.*, vol. 39, no. 1, pp. 327–335, Jan. 2018.
[36] S. K. Padhy, B. K. Panigrahi, P. K. Ray, A. K. Satpathy, R. P. Nanda, and A. Nayak, "Classification of faults in a transmission line using artificial neural network," in *Proc. Int. Conf. Inf. Technol. (ICIT)*, Dec. 2018, pp. 239–243.
[37] A. Osadchiy, A. Kamenev, V. Saharov, and S. Chernyi, "Signal processing algorithm based on discrete wavelet transform," *Designs*, vol. 5, no. 3, p. 41, Jul. 2021.
[38] P. Refaeilzadeh, L. Tang, H. Liu, L. Angeles, and C. D. Scientist, "Cross-validation," *Encyclopedia Database Syst.*, vol. 5, pp. 532–538, Jan. 2020.

KHALIL ALSHARABI received the B.S. degree in communication and computer engineering from Taiz University, Yemen, in 2008, and the M.S. degree in electrical engineering and control systems engineering from King Saud University, Saudi Arabia, in 2017, where he is currently pursuing the Ph.D. degree with the Department of Electrical Engineering. His research interests include brain–computer interfaces, EEG signal processing, control systems engineering, and artificial intelligence.

YASSER BIN SALAMAH received the M.S. and Ph.D. degrees from The Ohio State University (OSU), Columbus, OH, USA, in 2013 and 2019, respectively. He is currently an Assistant Professor in electrical engineering with King Saud University, Riyadh, Saudi Arabia. His research interests include optimization, intelligent control, artificial intelligence with application to autonomous systems, and renewable energy.

AKRAM M. ABDURRAQEEB received the B.S. degree in communication and computer engineering from Taiz University, Taiz, Yemen, in 2008, and the M.S. degree in automatic control from the Department of Electrical Engineering, King Saud University, Riyadh, Saudi Arabia, in 2017. He is currently pursuing the Ph.D. degree in automatic control with the Department of Electrical Engineering. His research interests include application of robust control for micro/nano-positioning systems, artificial intelligence, robotics, and EEG signal processing.

MAJID ALJALAL received the B.S. degree in communication engineering from Taiz University, Taiz, Yemen, in 2010, and the M.S. degree in electrical engineering from King Saud University, Riyadh, Saudi Arabia, in 2017, where he is currently pursuing the Ph.D. degree in electrical engineering with the Department of Electrical Engineering. His research interests include artificial intelligence, brain–computer interfaces, control systems, and EEG signal processing.

FAHD A. ALTURKI received the B.S. degree in electrical engineering from King Saud University, Riyadh, Saudi Arabia, in 1986, the M.S. degree in control systems from Imperial College, London, U.K., in 1988, and the Ph.D. degree in control engineering from Sheffield University, Sheffield, U.K., in 1993. He was the Dean of the College of Engineering (2008–2012), and has been the General Supervisor of King Saud University colleges, Almuzahimiah Branch, since April 2013. He is currently a Professor in electrical engineering with King Saud University. His research interests include intelligent systems, signal processing, and nonlinear control.